ChemComm

COMMUNICATION

View Article Online
View Journal | View Issue

Cite this: *Chem. Commun.*, 2016, 52, 12897

Received 17th September 2016,
Accepted 6th October 2016

DOI: 10.1039/c6cc07574f

www.rsc.org/chemcomm

A light-up imaging protocol for neutral pH-enhanced fluorescence detection of lysosomal neuraminidase activity in living cells†

Lei Bao,‡ Lin Ding,‡ Jingjing Hui and Huangxian Ju*

A lysosome-accessing nanoprobe is designed for recognition of lysosomal neuraminidases (Lyso-Neus), which can cleave the 4-methylumbelliferone moieties of the substrate from the nanoprobe, and lead to the escape of the moieties from acidic lysosomes into the neutral cytosol assisted by cationic poly(ethyleneimine) to light up the pH-responsive fluorescence for visual detection and dynamic tracking of Lyso-Neu activity in living cells.

Neuraminidases (Neus), also called sialidases, are a family of glycosidases responsible for removing α-glycosidically linked sialic acid (Sia) residues from glycoconjugates.[1] These enzymes are located at different cellular compartments such as lysosomes, the cytosol, the plasma membrane and mitochondria, and play a central role in regulating cell-surface Sia expression.[1b,2] Several fluorescence methods have been developed for the assay of plasma membrane-associated Neu activity by using 4-methylumbelliferyl-*N*-acetylneuraminic acid (4MUNA) and its derivatives as Neu-cleavable fluorogenic substrates.[3] A ganglioside-derived FRET probe has also been designed for ratiometric imaging of Neu activity on the surface of living cells.[4] However, detection methods dedicated for intracellular Neu activity, particularly lysosomal Neus (Lyso-Neus), are largely lacking despite the importance of Neus in controlling the desialylation of glycoproteins in lysosomes.

Lysosomes are terminal degradation compartments of the endocytic pathway, and can digest all major cellular macromolecules by different hydrolases, in which Lyso-Neus (including Neu1 and Neu4) can affect the expression of malignant phenotypes.[2,5] They display a down-regulated tendency in human colorectal cancers, and an up-regulation in the early stage of apoptosis.[6] The up-regulation accelerates the apoptosis and depression of invasion and motility. Currently available protocols for Lyso-Neu activity assay are limited to cell lysates, and cannot be employed for monitoring the activity change in living cells.[7] Although a cell-permeable probe has recently been designed to label intracellular Neus *via* irreversible binding, it fails to reflect the enzymatic cleavage activity.[8] Thus developing visualization methods for Lyso-Neu activity in living cells has become quite an urgent need.

The real-time visualization of Lyso-Neu activity faces three main challenges: (1) design of a Neu activity-responsive substrate, (2) efficient delivery of the Neu substrate to lysosomes, and (3) production of Neu-triggered "off–on" signals in living cells. Aiming at these challenges, this work proposed a cell-permeable and lysosome-accessing nanoprobe to efficiently deliver a Lyso-Neu-specific substrate into lysosomes and release the cleavage product into the cytosol for neutral pH-enhanced fluorescence detection of Lyso-Neu activity, which led to a light-up imaging strategy for monitoring of Lyso-Neu activity in living cells (Scheme 1). The efficient delivery was achieved using graphene oxide (GO) as the "carrier and locator" due to its high loading capability and endocytosis-mediated cellular internalization.[9] 4MUNA was assembled on the GO surface *via* a linker and could be specifically cleaved by Neus in acidic lysosomes (pH 5)[7] to produce a free 4-methylumbelliferone (4MU) moiety. The 4MU is pH-responsive and can yield strong fluorescence at neutral pH.[10] Thus, to facilitate the escape of the cleaved 4MU into the neutral cytosol for producing a strong signal, a cationic polymer, branched poly(ethyleneimine) (BPEI), was co-assembled on the GO surface,[11] which caused lysosomal osmotic swelling to form holes for escape of 4MU into the cytosol due to the unique proton-sponge effect.[12] The proposed light-up imaging strategy provided a powerful tool to track the dynamic variation of Lyso-Neu activity.

The Linker/GO composite was prepared by covalently conjugating 3-aminophenylboronic acid (APBA) to the succinimidyl end of 1-pyrenebutyric acid *N*-hydroxysuccinimide ester (PASE) that was pre-assembled on GO by π–π stacking.[13] The flexible alkyl chain in PASE was favorable for reducing the steric effect for recognition of the enzyme substrate. After BPEI was loaded onto the Linker/GO by electrostatic interaction, 4MUNA was

State Key Laboratory of Analytical Chemistry for Life Science, School of Chemistry and Chemical Engineering, Nanjing University, Nanjing 210023, P. R. China. E-mail: hxju@nju.edu.cn

† Electronic supplementary information (ESI) available: Materials, methods, characterization and supplementary data. See DOI: 10.1039/c6cc07574f

‡ These authors contributed equally to this work.

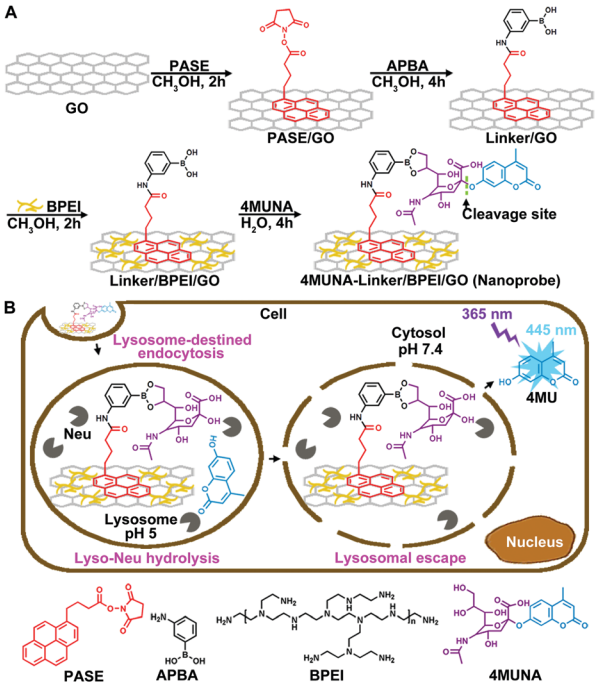

Scheme 1 Schematic illustration of (A) construction of the nanoprobe and (B) the light-up imaging strategy for Lyso-Neu activity in living cells.

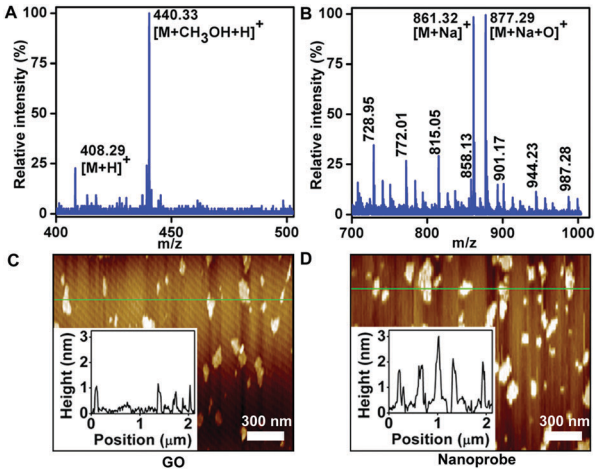

Fig. 1 Characterization of the nanoprobe. MALDI-TOF mass spectra of (A) Linker/GO and (B) the nanoprobe, and AFM images of (C) GO and (D) the nanoprobe. Insets: AFM height profiles recorded along the marked lines.

introduced by covalent binding of the *N*-acetylneuraminic acid (NA) moiety to the phenylboronic acid group of the linker to obtain the nanoprobe (Scheme 1A).[14] Using human colon tumor (HCT-15) cells as a model, the nanoprobe was efficiently taken up through clathrin-mediated endocytosis and transported to lysosomes.[9b,c] The Lyso-Neu-specific cleavage of 4MU followed by BPEI-assisted escape into the cytosol lightened up the fluorescence of 4MU for visual detection of Lyso-Neu activity (Scheme 1B). Moreover, the Neu associated with the cytosol did not interfere with the signal due to the trapping of the nanoprobe in lysosomes by the endocytic pathway.

The construction of the nanoprobe was confirmed by Fourier transform infrared (FT-IR), UV-vis and Zeta potential analysis (Fig. S1, ESI†). From the absorption peak of the nanoprobe at 315 nm, the loading amount of 4MUNA was determined to be 158 nmol mg^{-1} (Fig. S1D, ESI†). The formation of the Linker/GO and nanoprobe was further demonstrated by MALDI-TOF mass spectrometry. The two peaks at *m*/*z* of 440.33 and 408.29 were attributed to $[linker + CH_3OH + H]^{+13}$ and $[linker + H]^+$, respectively (Fig. 1A), considering the molecular weight of the linker ($C_{26}H_{22}BNO_3$, M = 407.27). The mass spectrum of the nanoprobe displayed two peaks at *m*/*z* of 877.29 and 861.32, and a series of peaks with an interval of 43 Da (Fig. 1B). The former was attributed to $[4MUNA\text{-}linker + Na]^+$ and $[4MUNA\text{-}linker + Na + O]^+$, respectively, and the latter corresponded to the repeat unit of CH_2CH_2NH in BPEI.[15] Here the molecular weight of the 4MUNA-linker ($C_{47}H_{43}BN_2O_{12}$) is 838.66. The atomic force microscopy (AFM) image showed single-layered dispersion of GO with a thickness of 0.7 nm and dimensions of around 200 nm (Fig. 1C). As a result of modification, the thickness of the nanoprobe increased to 1.5 nm (Fig. 1D).

The PASE acted not only as an assembly reagent for binding APBA but also as the fluorophore for indicating the location of the nanoprobe. Due to the overlap of the emissions of PASE and 4MU, the influence of the PASE amount on nanoprobe performance was first examined. At a PASE concentration of 0.05 mM for nanoprobe preparation, the addition of GO reduced the fluorescence of PASE efficiently (Fig. S2A, curves a and b, ESI†). After removing un-assembled PASE, the Linker/BPEI/GO showed negligible fluorescence of PASE (Fig. S2A, curve c, ESI†) due to the quenching of GO, while high PASE loading led to obvious fluorescent signals in both solution and living cells (Fig. S2, ESI†), indicating insufficient quenching of GO. Thus 0.05 mM PASE was used for preparation of the nanoprobe to avoid the influence of PASE fluorescence on Lyso-Neu activity detection, and 0.5 mM PASE was used for obtaining Linker/BPEI/GO as a tracker for colocalization of the internalized nanoprobe.

To improve the dispersion and stability of the nanoprobe in solution, BPEI with low molecular weight (M_w = 1.3 kDa) was exploited to functionalize GO, which not only alleviated cytotoxicity compared to that with higher molecular weight,[11] but also enhanced cellular uptake of the nanoprobe and lysosomal escape of cleaved 4MU due to the osmotic swelling for hole formation.[12] The concentration of BPEI used for GO coating was optimized by observation of the lysosomal morphology (Fig. S3, ESI†) and MTT assay (Fig. S4A, ESI†) of HCT-15 cells after 4 h incubation with Linker/BPEI/GO (10 μg mL^{-1}) prepared with different BPEI concentrations. 0.1 mM of BPEI was chosen to avoid the rupture of lysosomes and ensure good biocompatibility of the nanoprobe. To demonstrate the BPEI-assisted cellular uptake, the Linker/BPEI/GOs prepared with 0.5 mM PASE and different amounts of BPEI were used as trackers, which showed increased endocytic uptake of GO at higher BPEI concentration in HCT-15 cells after 4 h incubation measured by flow cytometric assay (Fig. S4B, ESI†); thus 0.1 mM BPEI was used for nanoprobe preparation.

After 4MUNA was incubated with commercial Neu in a mimic lysosomal environment, the hydrolysis product showed

~173 times (17 to 2945 a.u.) higher fluorescence at pH 7.4 than that at pH 5.0 (Fig. S5, ESI†), suggesting the pH-dependent fluorescence of the cleaved 4MU.[10] Only slight fluorescence (3 a.u. at pH 5.0 and 201 a.u. at pH 7.4) of 4MUNA in the absence of Neu was observed due to the quenching effect of NA on 4MU *via* the change in the mobility of π-electrons.[16] Thus 4MUNA was a favorable substrate for light-up detection of Lyso-Neu activity *via* the escape of cleaved 4MU into the cytosol to generate neutral pH-enhanced fluorescence. Moreover, the conjugation of APBA to 4MUNA did not obviously change the recognition by Neu and the cleavage of 4MU from the molecule (Fig. S6, ESI†).[17]

The specificity of the proposed nanoprobe to Neu was investigated using fluorescence measurements. The Neu activity at pH 5.0 was reported to be 5 fold that at pH 7.4.[7] After incubating the nanoprobe with Neu at pH 5.0, the fluorescence intensity (FI) was detected at pH 7.4. With increasing incubation time, the FI increased gradually, and tended to a plateau after 90 min (Fig. 2A), indicating complete cleavage of 4MU from the nanoprobe. The GO composite displayed a small effect (~11%) on the fluorescence signal of released 4MU (Fig. S7, ESI†). When the incubation mixture contained *N*-acetyl-2,3-dehydro-2-deoxyneuraminic acid (NADNA), a Neu inhibitor,[18] 2 h incubation did not produce the fluorescent signal of 4MU (Fig. 2B), indicating complete suppression of Neu activity. Thus the signal could be attributed to the specific cleavage activity of Neu. As a control, the Linker/BPEI/GO and the nanoprobe did not show any fluorescent signal (Fig. 2B), warranting a low background for highly sensitive detection of Neu activity. The hydrolyzed product on the nanoprobe was confirmed by MALDI-TOF mass spectroscopy to verify the cleavage of 4MU. The mass spectrum showed a peak at *m*/*z* of 703.74 (Fig. S8, ESI†), which was attributed to $[NA\text{-linker} + Na]^+$, considering that the molecular weight of the NA-linker ($C_{37}H_{37}BN_2O_{10}$) is 680.51. This result verified the release of 4MU from the nanoprobe.

The crude lysosomal lysate from HCT-15 cells was further used to examine the feasibility of the proposed Neu activity detection protocol. The Neu activity in 10 μL of crude lysosomal lysate (2.5×10^6 cells) was calculated to be 3.3×10^{-6} U, *i.e.* 1.0×10^6 HCT-15 cells contain 1.3×10^{-6} U Lyso-Neu (Fig. S9, ESI†).

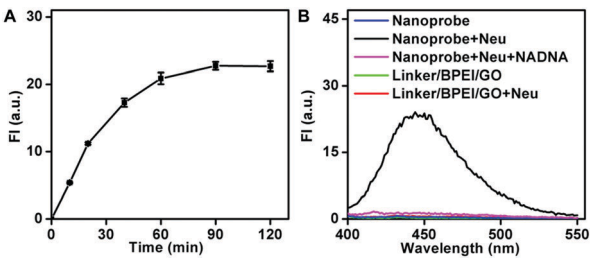

Fig. 2 (A) Fluorescence intensity of the nanoprobe (1 μg mL^{-1}, 158 nM 4MUNA equiv.) after being incubated with Neu (2 μU mL^{-1}) for different times at pH 5.0 and transferred to pH 7.4 buffer. (B) Fluorescence responses of Linker/BPEI/GO (1 μg mL^{-1}) and the nanoprobe (1 μg mL^{-1}, 158 nM 4MUNA equiv.) toward Neu, respectively. NADNA: a Neu inhibitor. λ_{ex} = 365 nm.

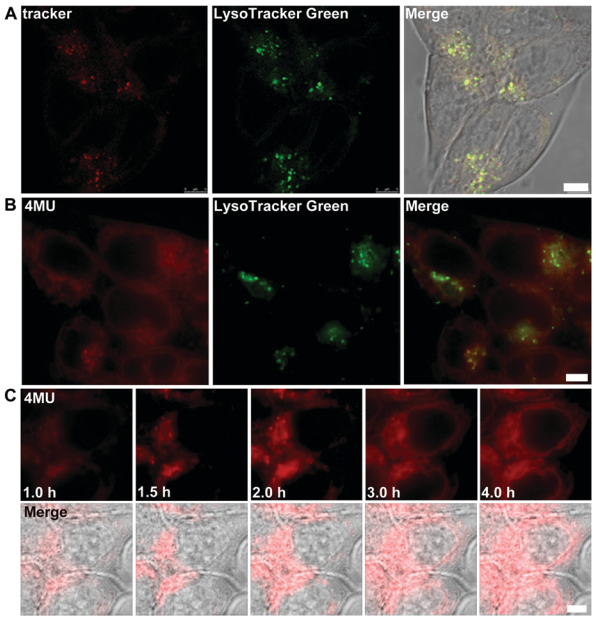

Fig. 3 Confocal images of HCT-15 cells after incubation with the (A) tracker and (B) nanoprobe for 4 h, respectively, followed by LysoTracker Green staining. (C) Fluorescence and bright field merged images of HCT-15 cells pretreated with NaBu for 48 h followed by incubation with a 10 μg mL^{-1} nanoprobe for marked times. Scale bars: 5 μm.

The stability of the nanoprobe was also investigated by soaking the nanoprobe in DMEM containing glucose and fetal bovine serum (FBS) at pH 5.0 and 7.4 to simulate the complex Neu-free lysosomal and cytosol environment, respectively. After the same Neu treatment, the soaked nanoprobe showed similar fluorescent signals, demonstrating good stability of the nanoprobe in living cells (Fig. S10, ESI†).

The entry of the nanoprobe into lysosomes was verified using a colocalization experiment. After 4 h incubation, the distribution of the tracker overlapped well with lysosomes stained with LysoTracker Green (Fig. 3A), suggesting that GO was a favorable carrier and locator for lysosomal sensing. After the living HCT-15 cells were incubated with the nanoprobe for 4 h, a strong fluorescent signal was observed in the cytoplasmic region, which overlapped with the stained lysosomes with only 6% of pixels (Fig. 3B), indicating the escape of released 4MU from acidic lysosomes to the neutral cytosol due to the proton-sponge effect of BPEI. This demonstrated the feasibility of the proposed light-up imaging strategy.

For the practical application of the imaging protocol, the incubation time of the nanoprobe was optimized with sodium butyrate (NaBu) treated HCT-15 cells, which induced the up-regulation of Lyso-Neu.[6,19] The fluorescence of 4MU unevenly appeared in the cytoplasmic region upon incubation up to 1.5 h, which showed some bright domains outside lysosomes (Fig. 3C). With increasing incubation time, the fluorescence expanded and became uniform in the cytoplasmic region, while the signal became brighter, indicating more 4MU molecules were cleaved from the nanoprobe and escaped to the cytosol. The maximum expansion and brightness occurred at an incubation time of 4 h.

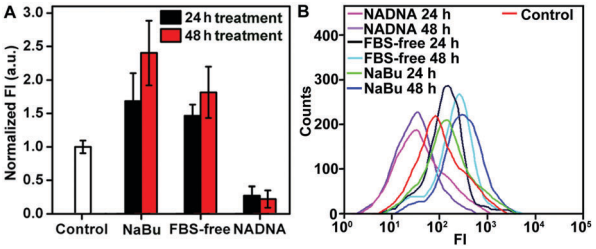

Fig. 4 Normalized mean FI of the cytoplasmic region (A) and flow cytometric analysis (B) of HCT-15 cells treated with NaBu-containing, FBS-free and NADNA-containing culture media for 24 h or 48 h, respectively, followed by incubation with the nanoprobe (10 μg mL^{-1}) for 4 h. Data are means ± SD (n = 3). Cells without treatment served as the control.

As a control, the cells with Lyso-Neus inhibited by NADNA presented much weaker fluorescence during the same incubation time (Fig. S11, ESI†). In addition, the cells showed 91% viability after 4 h incubation with a 10 μg mL^{-1} nanoprobe by MTT assay (Fig. S12, ESI†). These results further demonstrated that the nanoprobe was a powerful tool for visualization of Lyso-Neu activity in living cells.

The proposed strategy could be used to dynamically track the variation of Lyso-Neu activity in living cells during the apoptosis process and drug treatment by recording the mean FI of the cytoplasmic regions (Fig. 4A). The incubation of HCT-15 cells with FBS-free culture medium that induced cell apoptosis and NaBu-containing culture medium increased Lyso-Neu activity by 1.5 and 1.7 times at 24 h and 1.8 and 2.4 times at 48 h, respectively. These results were in good agreement with the fact that Lyso-Neu activity could be up-regulated in the early stage of apoptosis induced by NaBu or FBS-free treatment.[6] In response to the Neu inhibitor, NADNA, the Lyso-Neu activity decreased to 27% and 22% after being treated for 24 and 48 h, respectively, suggesting obvious inhibition effects. These results were further verified by flow cytometric assays (Fig. 4B) and were consistent with the data obtained from crude lysosomal lysates (Fig. S13, ESI†). As a control, a flow cytometric experiment was also performed by monitoring the fluorescence of cells after being incubated with only 4MUNA or Linker/BPEI/GO. These cells did not show any increase of the fluorescence signal (Fig. S14, ESI†), suggesting a negligible background and eliminating the interference from cell surface Neus. These data also demonstrated the necessity of using Linker/BPEI/GO to deliver 4MUNA toward lysosomes[3b] for highly sensitive imaging of Lyso-Neu activity in living cells.

In conclusion, a light-up imaging strategy has been developed for specific visualization of Lyso-Neu activity in living cells with neutral pH-enhanced fluorescence emission. The newly designed lysosome-accessing nanoprobe is prepared by assembling 4MUNA and BPEI on the Linker/GO surface. The nanoprobe can be efficiently delivered to lysosomes and specifically recognized by Lyso-Neus. The presence of cationic BPEI contributes to lysosomal osmotic swelling to form holes on the lysosomal membrane. The enzymatic cleavage of 4MU moieties from the nanoprobe in acidic lysosomes and the subsequent escape from lysosomes to the neutral cytosol lead to light-up fluorescent signals. The advantages of the designed nanoprobe warrant its excellent performance for *in situ* tracing of Lyso-Neu activity in living cells. The proposed strategy has been employed for monitoring the changes of Lyso-Neu activity in the cell apoptosis process and in response to drugs. We anticipate that this strategy can accelerate the understanding of the biological roles of Neus in cancer, and provide a valuable tool for discovery of novel Neu-related drugs.

We acknowledge the financial support of the National Natural Science Foundation of China (21135002, 21635005, 21675082, 21322506) and the National Basic Research Program (2014CB744501).

Notes and references

1 (*a*) M. Fukuda and X. Bao, *Nat. Chem. Biol.*, 2008, **4**, 721–722; (*b*) O. M. Pearce and H. Laubli, *Glycobiology*, 2016, **26**, 111–128.
2 T. Miyagi, K. Takahashi, K. Shiozaki and K. Yamaguchi, in *Sugar Chains: Decoding the Functions of Glycans*, ed. T. Suzuki, K. Ohtsubo and N. Taniguchi, Springer, Japan, Tokyo, 2015, pp. 159–176.
3 (*a*) M. Potier, L. Mameli, M. Bélisle, L. Dallaire and S. B. Melançon, *Anal. Biochem.*, 1979, **94**, 287–296; (*b*) C. Y. Zamora, M. d'Alarcao and K. Kumar, *Bioorg. Med. Chem. Lett.*, 2013, **23**, 3406–3410; (*c*) Y. Kurebayashi, T. Takahashi, T. Otsubo, K. Ikeda, S. Takahashi, M. Takano, T. Agarikuchi, T. Sato, Y. Matsuda, A. Minami, H. Kanazawa, Y. Uchida, T. Saito, Y. Kawaoka, T. Yamada, F. Kawamori, R. Thomson, M. von Itzstein and T. Suzuki, *Sci. Rep.*, 2014, **4**, 4877.
4 G. Y. Yang, C. Li, M. Fischer, C. W. Cairo, Y. Feng and S. G. Withers, *Angew. Chem., Int. Ed.*, 2015, **54**, 5389–5393.
5 G. Kroemer and M. Jaattela, *Nat. Rev. Cancer*, 2005, **5**, 886–897.
6 (*a*) Y. Kakugawa, T. Wada, K. Yamaguchi, H. Yamanami, K. Ouchi, I. Sato and T. Miyagi, *Proc. Natl. Acad. Sci. U. S. A.*, 2002, **99**, 10718–10723; (*b*) H. Yamanami, K. Shiozaki, T. Wada, K. Yamaguchi, T. Uemura, Y. Kakugawa, T. Hujiya and T. Miyagi, *Cancer Sci.*, 2007, **98**, 299–307.
7 T. Miyagi and S. Tsuiki, *Eur. J. Biochem.*, 1984, **141**, 75–81.
8 C.-S. Tsai, H.-Y. Yen, M.-I. Lin, T.-I. Tsai, S.-Y. Wang, W.-I. Huang, T.-L. Hsu, Y.-S. E. Cheng, J.-M. Fang and C.-H. Wong, *Proc. Natl. Acad. Sci. U. S. A.*, 2013, **110**, 2466–2471.
9 (*a*) Y. Liu, X. Dong and P. Chen, *Chem. Soc. Rev.*, 2012, **41**, 2283–2307; (*b*) J. Huang, C. Zong, H. Shen, M. Liu, B. Chen, B. Ren and Z. Zhang, *Small*, 2012, **8**, 2577–2584; (*c*) Q. Mu, G. Su, L. Li, B. O. Gilbertson, L. H. Yu, Q. Zhang, Y. P. Sun and B. Yan, *ACS Appl. Mater. Interfaces*, 2012, **4**, 2259–2266.
10 J. A. R. Mead, J. N. Smith and R. T. Williams, *Biochem. J.*, 1955, **61**, 569–574.
11 (*a*) L. Feng, S. Zhang and Z. Liu, *Nanoscale*, 2011, **3**, 1252–1257; (*b*) H. Kim, R. Namgung, K. Singha, I. K. Oh and W. J. Kim, *Bioconjugate Chem.*, 2011, **22**, 2558–2567.
12 A. E. Nel, L. Madler, D. Velegol, T. Xia, E. M. V. Hoek, P. Somasundaran, F. Klaessig, V. Castranova and M. Thompson, *Nat. Mater.*, 2009, **8**, 543–557.
13 L. Zhang, Y. Cheng, J. P. Lei, Y. T. Liu, Q. Hao and H. X. Ju, *Anal. Chem.*, 2013, **85**, 8001–8007.
14 H. Otsuka, E. Uchimura, H. Koshino, T. Okano and K. Kataoka, *J. Am. Chem. Soc.*, 2003, **125**, 3493–3502.
15 E. Rivera-Tirado and C. Wesdemiotis, *J. Mass Spectrom.*, 2011, **46**, 876–883.
16 R. Giri, S. S. Rathi, M. K. Machwe and V. V. S. Murti, *Spectrochim. Acta, Part A*, 1988, **44**, 805–807.
17 Z. Khedri, M. M. Muthana, Y. Li, S. M. Muthana, H. Yu, H. Cao and X. Chen, *Chem. Commun.*, 2012, **48**, 3357–3359.
18 C. W. Cairo, *MedChemComm*, 2014, **5**, 1067–1074.
19 C. Augeron and C. L. Laboisse, *Cancer Res.*, 1984, **44**, 3961–3969.

